Extracellular thiol-assisted selenium uptake dependent on the x_c^- cystine transporter explains the cancer-specific cytotoxicity of selenite

Eric Olm[a,1], Aristi P. Fernandes[a], Christina Hebert[b], Anna-Klara Rundlöf[a], Erik H. Larsen[c], Olof Danielsson[a], and Mikael Björnstedt[a,1]

[a]Division of Pathology F46, Department of Laboratory Medicine, Karolinska Institutet and [b]Division of Anesthesiology and Intensive Care, Department of Clinical Sciences, Intervention and Technology (CLINTEC), Karolinska University Hospital Huddinge, KFC Novum, Stockholm SE-141 86, Sweden and [c]Department of Food Chemistry, Technical University of Denmark, National Food Institute, DK-2860 Søborg, Denmark

Edited by Jan-Ake Gustafsson, Karolinska Institutet, Huddinge, Sweden, and approved May 13, 2009 (received for review March 2, 2009)

The selenium salt selenite (SeO_3^{2-}) is cytotoxic in low to moderate concentrations, with a remarkable specificity for cancer cells resistant to conventional chemotherapy. Our data show that selenium uptake and accumulation, rather than intracellular events, are crucial to the specific selenite cytotoxicity observed in resistant cancer cells. We show that selenium uptake depends on extracellular reduction, and that the extracellular environment is a key factor specific to selenite cytotoxicity. The extracellular reduction is mediated by cysteine, and the efficacy is determined by the uptake of cystine by the x_c^- antiporter and secretion of cysteine by multidrug resistance proteins, both of which are frequently overexpressed by resistant cancer cells. This mechanism provides molecular evidence for the existence of an inverse relationship between resistance to conventional chemotherapy and sensitivity to selenite cytotoxicity, and highlights the great therapeutic potential in treating multidrug-resistant cancer.

drug resistance | pharmacology | selenium

Selenite (SeO_3^{2-}) efficiently inhibits the growth of malignant cells and studies suggest an inverse relationship between resistance to cytotoxic drugs and sensitivity to selenite (SeO_3^{2-}) (1, 2). A major mechanism of selenite cytotoxicity is thought to be the generation of oxidative stress through intracellular redox cycling of the selenium metabolite selenide with oxygen and cellular thiols, producing nonstoichiometric amounts of superoxide and cellular disulfides. The induction of oxidative stress and consequent apoptosis has been demonstrated in numerous cancer cell lines (2–8), but why this occurs only in malignant cells at easily achievable selenium plasma concentrations remains unclear.

With the assumption that the mechanistic explanation is intracellular, studies on differences in cellular uptake have been neglected. Already in the 1960s, selenite (SeO_3^{2-}) was being used experimentally as a tumor-localizing agent. Neoplasms could be detected in brain and thorax in human subjects through i.v. administration of radioactive selenite (^{75}Se) (9). Although at that time the cancer-specific cytotoxic effects of selenite were unknown, and low doses were used (approximately in the nM range in blood) (9), early findings clearly demonstrated that cancer cells enrich selenium in vivo. These findings, combined with current knowledge of selenite's toxic effects on malignant cells, raise the possibility of a cancer-specific high-affinity selenium uptake mechanism that might explain cancer-specific selenite cytotoxicity at therapeutic selenite concentrations (μM range).

In yeast, millimolar tolerance to selenite can be reduced to the micromolar range by the presence of excessive thiols in the growth medium through high-affinity uptake of a more reduced form of selenite, possibly selenide (10). High-affinity uptake of selenium through the addition of extracellular thiols also has been demonstrated in a keratinocyte model (11) using nanomolar concentrations of selenite. Selenium uptake was prevented in keratinocytes by the anion channel blocker 4,4′-diisothiocyanostilbene-2,2′-disulphonic acid (DIDS) in the presence and absence of glutathione (GSH), suggesting that both selenite and selenide were taken up through these pathways but with different affinities.

The x_c^- cystine/glutamate antiporter facilitates the uptake of extracellular cystine in exchange for intracellular glutamate, and is widely expressed in different cancer cell lines as well as primary tumors (reviewed in ref. 12). The availability of cysteine is the limiting step in GSH synthesis (13), and thus high cysteine availability is also important in the cellular defense against oxidative stress and may aid drug resistance. In extracellular plasma, cysteine levels are low ($\approx$10 μM), and cystine levels are almost 10-fold higher (14), giving x_c^--expressing cancer cells access to a larger pool of cysteine. Overexpression of the x_c^- transport system in the HH514 Burkitt's lymphoma cell line was recently reported to have only limited impact on intracellular GSH levels but to drive a cystine/cysteine redox cycle resulting in high extracellular cysteine levels, thereby protecting the extracellular compartment from oxidative stress (15).

The goal of the present study was to explore the connections among selenium uptake, selenite cytotoxicity, and the redox state of the microenvironment. We hypothesized that a reducing microenvironment dependent on the x_c^- antiporter could lead to a high-affinity selenium uptake that might explain cancer cell–specific selenite cytotoxicity.

Results

Selenite Cytotoxicity Is Determined by Selenium Uptake. We used 3 lung cancer cell lines with varying selenite sensitivity to explore the relationship between selenium uptake and selenite cytotoxicity [supporting information (SI) Table S1]. Uptake was measured in cells treated with a dose of 5 μM for 5 h to explore whether selenium accumulation preceded cytotoxicity. The dose was chosen to be suitable for cells with varying sensitivity to selenite, including highly toxic (H157), borderline toxic (U2020), and nontoxic (H611). Selenium accumulation was greatest in the H157 cells (280 ± 6 ng/mg total protein), less in the U2020 cells (60 ± 9 ng/mg total protein), and undetectable in the H611 cells. These results correspond closely to the toxicity at the given doses and suggest that selenite toxicity is determined by the level of selenium accumulation in cells.

Author contributions: E.O., A.P.F., O.D., and M.B. designed research; E.O., C.H., and E.H.L. performed research; E.O., A.P.F., A.-K.R., O.D., and M.B. analyzed data; and E.O., O.D., and M.B. wrote the paper.

The authors declare no conflict of interest.

This article is a PNAS Direct Submission.

[1]To whom correspondence may be addressed. E-mail: eric.olm@ki.se or mikael.bjornstedt@ki.se.

This article contains supporting information online at www.pnas.org/cgi/content/full/0902204106/DCSupplemental.

www.pnas.org/cgi/doi/10.1073/pnas.0902204106

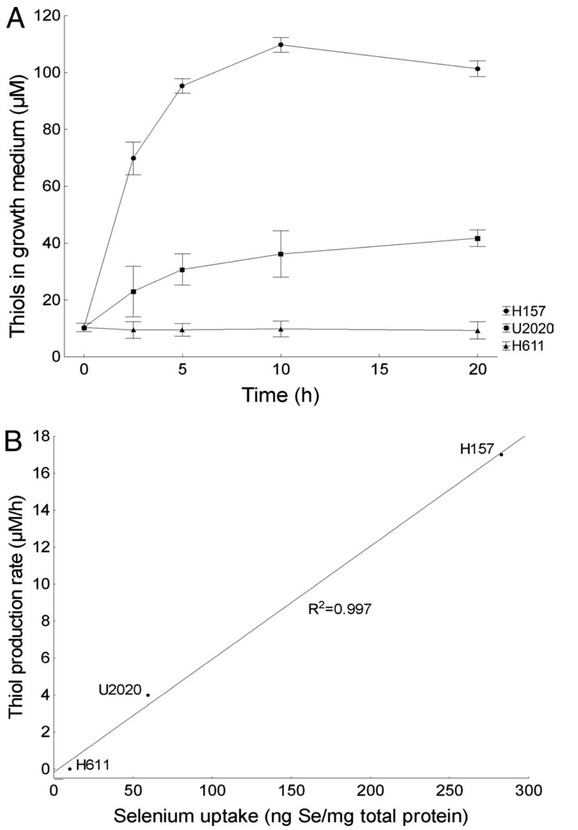

Fig. 1. Selenite sensitivity is related to selenium uptake and extracellular thiols. Error bars display ± 0.95 confidence intervals. (*A*) Extracellular thiols, produced by cells at 0–20 h, measured with DTNB. (*B*) Total selenium uptake in cells treated with 5 μM selenite at 5 h measured with inductively coupled plasma mass spectroscopy, correlated to extracellular thiol production rate at 5 h measured with DTNB.

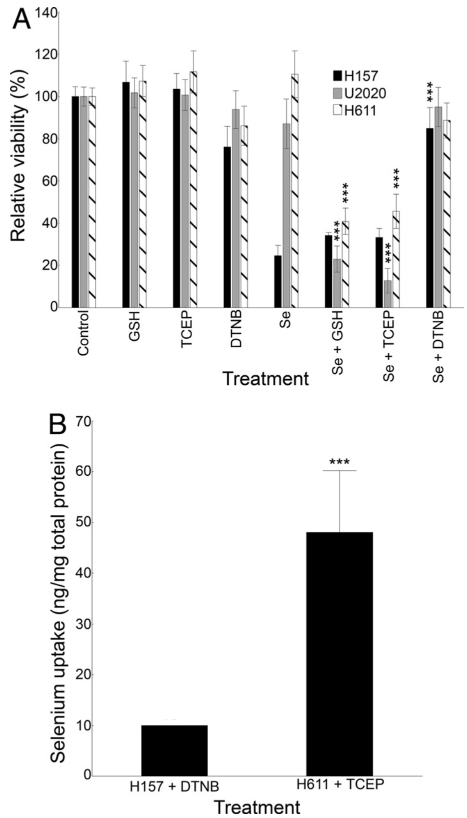

Fig. 2. Modulation of the extracellular redox state alters selenite sensitivity and selenium uptake. Error bars display ± 0.95 confidence intervals. ***$P <$ .001. (*A*) Viability measured by XTT in lung cancer cells treated with 5 μM selenite for 20 h. GSH (75 μM) and TCEP (75 μM) were used as extracellular reductants. DTNB (500 μM) was used as an extracellular thiol scavenger. *In relation to selenite treatment. (*B*) Total selenium uptake, measured at 5 h, in extracellular redox state–modulated cells treated with 5 μM selenite and TCEP (75 μM) in H611 cells or DTNB (500 μM) in H157 cells.

Selenium Uptake Is Dependent on the Extracellular Redox State. To explore the connection between selenium uptake and the extracellular redox state, we measured the total production of extracellular thiols from the cells over time (Fig. 1*A*). Extracellular thiol production was highest in the H157 cells, peaking at ≈110 μM at 10 h, and was lower in the U2020 cells, peaking at ≈40 μM at 20 h. Production in the H611 cells did not differ significantly from that seen in the control growth medium (≈10 μM). Extracellular thiol production showed a remarkable correlation with selenium uptake measured previously ($R^2 = 0.997$) (Fig. 1*B*), suggesting a strong relationship between a reductive microenvironment and high-affinity selenium uptake.

To verify this relationship and its connection to cytotoxicity, we artificially redox-modulated the extracellular compartment and treated the cells with 5 μM selenite. Viability measured at 20 h was used as an endpoint. Extracellular reduction through inclusion of the cell-impermeable reductants GSH or Tris(2-carboxyethyl)phosphine (TCEP) led to increased selenite toxicity at equal concentrations (75 μM) (Fig. 2*A*). Conversely, 500 μM 55′-dithiobis-(2-nitrobenzoic acid) (DTNB) used as a cell-impermeable oxidant or thiol scavenger protected the cells from any toxic effects of selenite compared with the DTNB control. Additional experiments also showed that the presence of DTNB increased the IC-50 for selenite from ≈4 μM to ≈40 μM in the sensitive H157 cells.

To confirm that the increase in selenite sensitivity was due to a change in actual selenium uptake, we measured the selenium content in the highly sensitive H157 cells after treatment with DTNB and selenite and in the resistant H611 cells after treatment with TCEP and selenite (Fig. 2*B*). The results clearly validate that the innate extracellular reductive capacity is crucial for selenite cytotoxicity and is mediated by an extracellular thiol–dependent high-affinity uptake mechanism.

The Major Part of Extracellular Thiols Is Cysteine. Protein precipitation of growth medium from the cells suggests that the dominant part of extracellular thiols is composed of low–molecular weight compounds (data not shown). To characterize these compounds, we measured the reduced/total cysteine and GSH content over time using HPLC. The greatest increase in extracellular levels of reduced cysteine over time was seen in the H157 cells (peaking at ≈100 μM in the growth medium at 10 h), followed by the U2020 cells (≈30 μM), and then the H611 cells (≈5 μM) (Fig. 3*A*). The consumption rate of total medium cystine/cysteine also was highest in the H157 cells, followed by the U2020 cells and then the H611 cells. Extracellular levels of reduced GSH were enhanced in both the H157 (≈6 μM at 20 h) and U2020 cells (≈3 μM at 20 h), but remained low in all 3 cell lines compared with cysteine levels (Fig. 3*B*).

Extracellular Thiol Production and, Consequently, Selenium Uptake and Cytotoxicity Are Dependent on Cystine Uptake Through the x_c^- Cystine Antiporter. Because of the x_c^- antiporter's potential to mediate a reduced extracellular environment, along with its frequent and broad expression in different malignancies, we explored the antiporter's role in the differing extracellular redox states. We initially performed Western blot analysis to detect any major

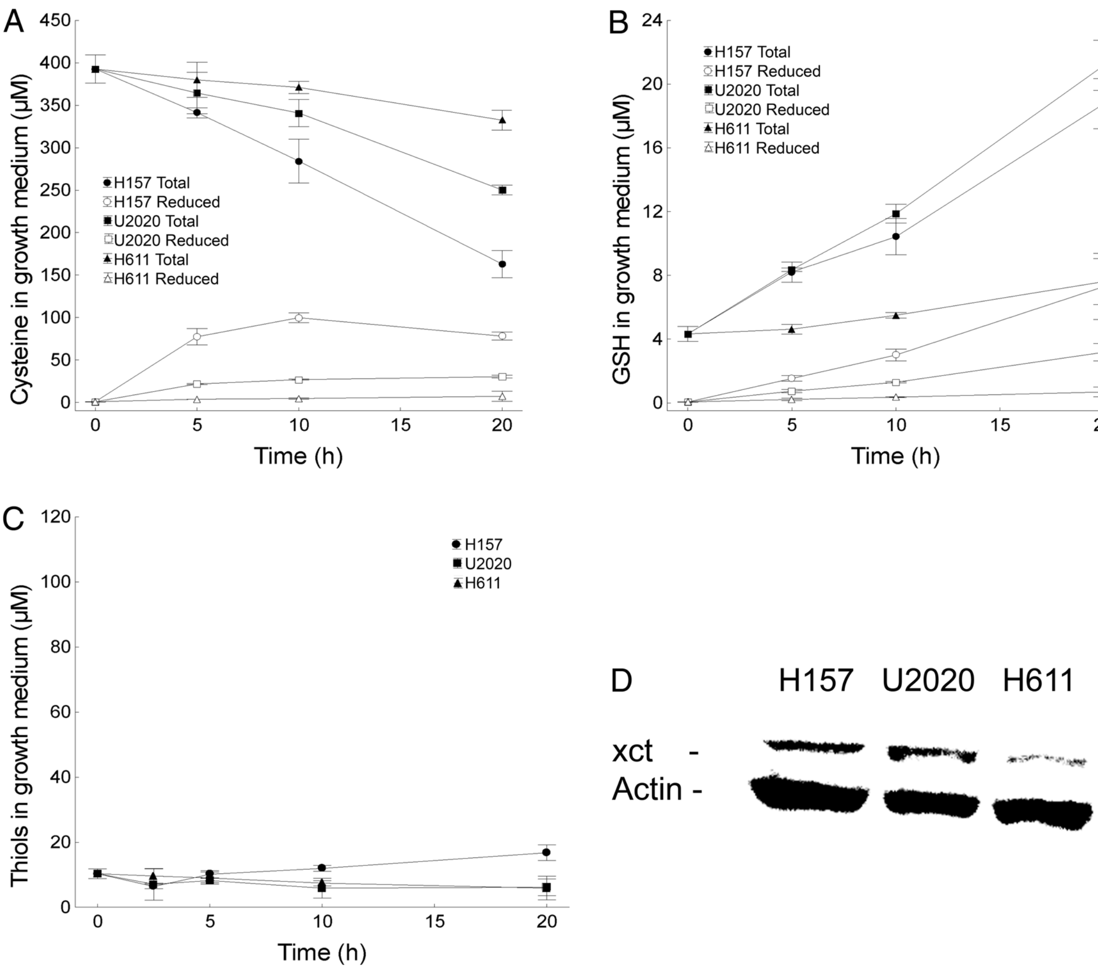

Fig. 3. Lung cancer cells expressing the x_c^- cystine/glutamate antiporter have a reduced extracellular microenvironment, mainly through cysteine secretion. Error bars display ± 0.95 confidence intervals. (*A*) Total growth medium cystine/cysteine levels and reduced cysteine levels in lung cancer cells at 0–20 h, measured with HPLC. (*B*) Total growth medium reduced/oxidized glutathione levels and reduced glutathione levels in lung cancer cells at 0–20 h, measured with HPLC. (*C*) Total extracellular thiol levels in cells treated with monosodium glutamate (60 mM) at 0–20 h. (*D*) Western blot analysis of the x_c^- cystine/glutamate antiporter–specific xct subunit. Actin was used as a loading control.

differences in expression. The x_c^- antiporter was expressed more markedly in both selenite-sensitive cell lines compared with the selenite-resistant H611 cell line (Fig. 3*D*). To explore whether the antiporter activity is involved in mediating a reduced extracellular compartment, we used monosodium glutamate (MSG) to readily and specifically inhibit the x_c^- antiporter (16). Adding MSG to the growth medium inhibited production of thiols in a dose-dependent manner (data not shown), and at 60 mM, MSG inhibited secretion of almost all thiols from the cell lines investigated (Fig. 3*C*) (compare with Fig. 1*A* for untreated cells). The data support an absolute dependence on cystine uptake through the x_c^- antiporter in the secretion of thiols, mainly cysteine, to the extracellular compartment.

To verify that inhibition of the x_c^- antiporter and, consequently, of cysteine secretion protects cells from selenite cytotoxicity, we treated cells with MSG and selenite. We found that MSG protected the cells from any toxic effects of selenite, an effect that could be reestablished by artificial reduction of the extracellular compartment (Fig. 4*A*). This demonstrates that it is not the inhibition of the antiporter per se, but rather the resulting cessation of thiol secretion, that causes decreased cytotoxicity. The changes in cytotoxicity with MSG in the sensitive H157 cell line were found to result from the inhibition of selenium uptake (Fig. 4*B*). Additional experiments also demonstrated that MSG shifted the IC-50 from ≈4 μM to ≈20 μM in the H157 cells, comparable to the IC-50 in the tolerant H611 cells.

The Multidrug Resistance Protein Efflux Pumps Are Involved in Cysteine Secretion. We used 2 competitive inhibitors, at nontoxic doses, to explore possible secretory pathways of reduced cysteine: MK571, an inhibitor of the multidrug resistance protein (MRP) family, and verapamil, an inhibitor of P-glycoprotein (Pgp). Verapamil had no significant effect on thiol secretion, but treatment with MK571 resulted in decreased extracellular thiol levels in a dose-dependent manner, as expected of a competitive inhibitor (Fig. 5*A* and *B*).

Cytotoxicity of Both Seleno-Di-Glutathione and Selenocystine Are Inhibited by DTNB and MSG. We also tested the redox active selenium compounds seleno-di-glutathione (GSSeSG) and selenocystine combined with DTNB and MSG in the H157 cells. GSSeSG was more toxic than selenite (data not shown), but its toxicity was significantly inhibited by DTNB and MSG, suggesting that reduction is required for uptake (Fig. S1*B*). Selenocystine was less potent than selenite or GSSeSG (data not shown) but also was significantly inhibited by DTNB and MSG at toxic levels (Fig. S1*A*), suggesting that it is taken up either in its reduced form as selenocysteine or as a selenocys-cysteine con-

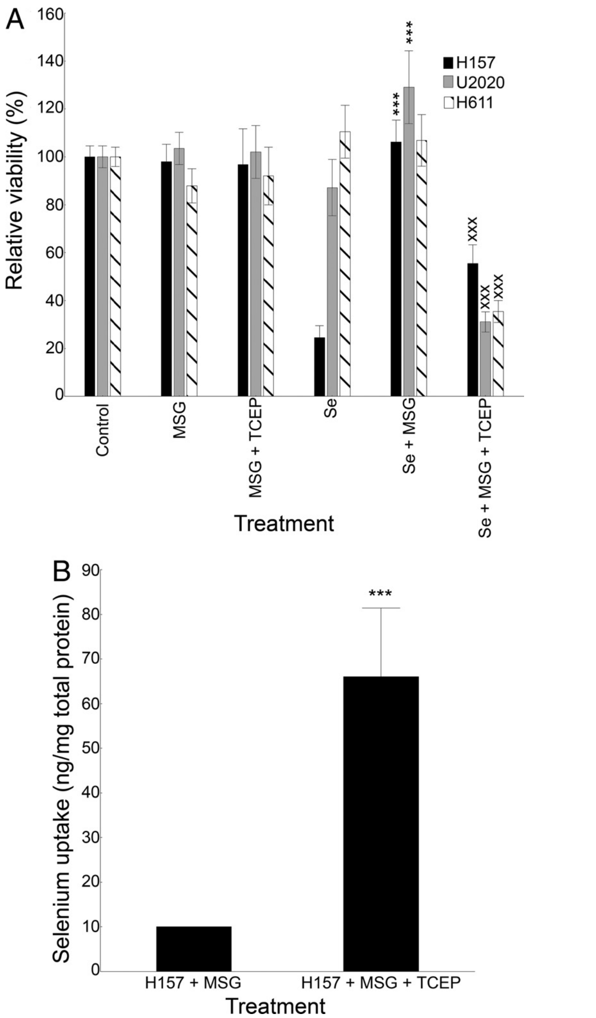

Fig. 4. Inhibition of the x_c^- cystine/glutamate antiporter inhibits selenium uptake and selenite toxicity. Error bars display ± 0.95 confidence intervals. ***(xxx)$P < .001$ (*A*) Viability measured by XTT in lung cancer cells treated with 5 μM selenite for 20 h. MSG (60 mM) was used as an inhibitor of the x_c^- cystine/glutamate antiporter, and TCEP (75 μM) with MSG was used as an extracellular thiol impact control. *In relation to selenite treatment; [x]In relation to selenite + MSG. (*B*) Total selenium uptake, measured at 5 h, in H157 cells treated with 5 μM selenite with MSG or with MSG + TCEP.

jugate (CysSe-Cys) through the x_c^- antiporter. These results indicate that our findings are general and apply to at least 3 common redox active forms of selenium.

The Uptake/Cytotoxicity Mechanism Is General and Not Limited to Lung Cancer Cells. To explore whether our findings can be generalized, we tested cancer cell lines of different origins in a XTT [sodium 3′-[1-(phenylaminocarbonyl)- 3,4-tetrazolium]-bis (4-methoxy-6-nitro) benzene sulfonic acid hydrate] viability panel with selenite combined with TCEP, DTNB, MSG, or MSG + TCEP. Hepatoma (HUH7) and neuroblastoma (SH5YSY) cell lines were used (Fig. S2). The neuroblastoma cells, with an extracellular redox status similar to that of the resistant H611 cells, were highly resistant. In the hepatoma cells, which had an extracellular redox status similar to that of the U2020 cells, selenite was borderline toxic at given doses. TCEP markedly increased the toxicity of selenite in both cell lines, whereas DTNB inhibited all toxic effects. MSG also inhibited the toxic effects of selenite, but these effects were reestablished in combination with TCEP. These results are consistent with the findings in the lung cancer cells.

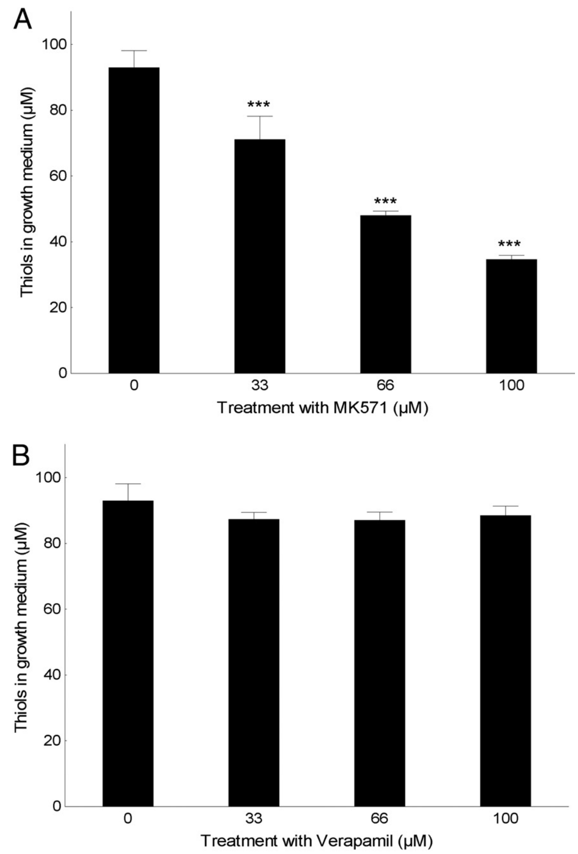

Fig. 5. MRP, but not Pgp, is involved in cysteine secretion from lung cancer cells. Error bars display ± 0.95 confidence intervals. ***$P < .001$ in relation to no inhibitor. (*A*) Extracellular redox state measured with DTNB at 5 h in H157 cells treated with/without the MRP-specific inhibitor MK571. (*B*) Extracellular redox state measured with DTNB at 5 h in H157 cells treated with/without the Pgp-specific inhibitor verapamil.

Discussion

Drug-resistant tumor cells have been shown to be particularly sensitive to selenite toxicity, with growth-inhibiting effects observed at low concentrations harmless to cell type– or patient-matched normal cells (2, 17). The mechanisms behind this specificity remain unclear, however. To investigate the role of extracellular thiols in selenite toxicity, we treated cell lines of varying sensitivity with selenite and investigated the extracellular redox state, selenium uptake, and the expression and involvement of the x_c^- cystine/glutamate antiporter. We found a clear association between extracellular thiols and selenite sensitivity and selenium uptake, which was verified by artificial redox modulation of the extracellular compartment. Furthermore, we found that the innate extracellular thiols were composed mainly of secreted cysteine through MRPs, driven by cystine uptake through the x_c^- antiporter. Our findings clearly demonstrate that x_c^- antiporter expression with concomitant secretion of cysteine, mainly through MRPs, is associated with selenite sensitivity, and that this is mediated through a high-affinity uptake by a reduced form of selenite.

Scintigraphic studies from the 1960s and 1970s demonstrated that selenium, administered i.v. as selenite, was enriched in cancer cells. In a study by Cavalieri et al. (9), patients with tumors of the brain and chest were scanned, and all brain tumors were correctly localized with selenite. Selenium was enriched 10- to 13-fold compared with normal brain tissue, and positive scans were achieved as early as 4 h after injection, suggesting a high-affinity uptake. The x_c^- antiporter has been particularly associated with brain tumors, in which glutamate release also might be involved in destruction of neuronal tissue during tumor invasion (18); for example, the x_c^- antiporter was prominently expressed in all samples derived from 5 glioma patients (19). Furthermore, sodium selenite has been shown to induce superoxide-mediated mitochondrial damage and subsequent autophagic cell death in 3 malignant glioma cell lines (20). The in vivo enrichment of selenium in brain tumors, expression of the x_c^- antiporter in vivo and in cell lines, and the prominent pro-apoptotic effects of selenite in glioma cell lines are most likely linked to, and explained by, our findings.

X_c^- antiporter expression has been increasingly connected to tumor growth and drug resistance (15, 21, 22) and has been shown to be regulated by the antioxidant response element (ARE) (23). Activation of the ARE induces several proteins known as phase II proteins, including MRPs plus enzymes regulating intracellular redox homeostasis. These proteins mediate cellular detoxification and protection from oxidative stress, but also are associated with drug resistance in cancer cells. The role of the x_c^- antiporter among the ARE-regulated proteins is to facilitate uptake of cystine, increasing intracellular cysteine availability and thereby enhancing GSH levels, which is important in drug resistance and the cellular defense against oxidative stress.

Although the x_c^- antiporter and related ARE-regulated proteins have been suggested as drug targets to reinduce chemotherapy sensitivity, our findings demonstrate that selenite cytotoxicity actually depends on the expression of these proteins. This suggests a possible relationship between selenite sensitivity and conventional drug resistance, which we indeed noted in our cell lines. We found that the H157 and U2020 cell lines, which prominently expressed the x_c^- antiporter, were the most sensitive to selenite, whereas the H611 cell line was highly selenite-resistant. Conversely, H611 was doxorubicin-sensitive, and H157 and U2020 were doxorubicin-resistant (data not shown). An inverse relationship has been demonstrated in lung cancer cells in a study exploring the effects on cellular redox protein thioredoxin reductase (TrxR) in the context of selenite treatment (1). In that study, 3 parental drug–sensitive cell lines were used with doxorubicin-resistant sublines. In 2 cases, the doxorubicin-resistant sublines were significantly more sensitive to selenite than their parental counterparts. Interestingly, in both of those cases, the drug resistance was conferred by MRP overexpression, whereas in the third subline, with similar selenite sensitivity as its parental cell line, drug resistance was conferred by Pgp. These findings are consistent with our results suggesting MRP, but not Pgp, as a secretory pathway of reduced cysteine. The roles of the ARE element and upstream regulators, such as Nrf2 (24), in selenite cytotoxicity merit investigation.

Thiol secretion from cancer cells has been reported previously but is poorly characterized. Ceccarelli et al. (25) recently reported that secretion of nonprotein thiols from lung cancer cells affects tumor progression and response to pro-oxidants. They also demonstrated a dependence of thioredoxin 1 (Trx1) on levels of secreted nonprotein thiols. Trx1 is a NADPH-dependent redox protein (via thioredoxin reductase) that reduces intracellular disulfides, including cystine, and thus may be involved as an intracellular limiting factor in the cystine/cysteine redox cycle. But almost complete inhibition of Trx1 protein expression with siRNA did not decrease the secretion of extracellular nonprotein thiols by 50% compared with control cells, indicating dependence on other redox molecules also capable of direct or indirect cystine reduction (possibly GSH, glutathione reductase, thioredoxin reductase, and glutaredoxins). Because of their mutual NADPH dependence (via glutathione reductase and thioredoxin reductase), levels of NADPH and NADPH-regenerating enzymes, such as NADPH dehydrogenase, also must be considered. Thus the intracellular redox systems' impact on extracellular thiols and possible dual role in selenite cytotoxicity, also being protective against intracellular oxidative stress, merits further investigation. This complexity may explain the findings of Shen et al. (26), who, in an effort to understand selenite cytotoxicity in connection with intracellular redox status, modulated GSH levels in hepatoma cells. Both increasing and decreasing intracellular glutathione levels sensitized the cells to selenite. Another interesting previously unexplained finding of Shen et al. (26) is that adding reduced GSH together with selenite extracelluarly produced the greatest increase in cytotoxicity, an effect likely explained by our model.

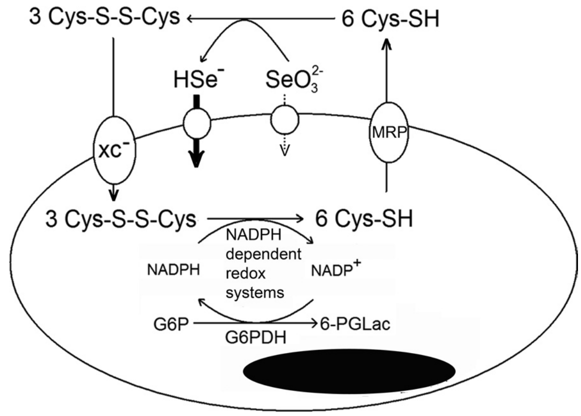

Fig. 6. Model for selenite cytotoxicity. The x_c^- cystine/glutamate antiporter facilitates the uptake of cystine, which is reduced intracellularly to cysteine by NADPH-dependent redox systems. A significant fraction of intracellular cysteine is resecreted into the extracellular compartment by MRPs, causing a reductive extracellular microenvironment. Extracellular reduction of selenite leads to a high-affinity uptake of a reduced form of selenite, possibly selenide, causing selenium accumulation and toxicity.

Control experiments revealed that the redox active selenium compounds seleno-L-cystine and GSSeSG also are dependent on extracellular thiols for cytotoxicity. The toxicity of GSSeSG was comparable to that of selenite, likely reflecting the efficient reduction to selenide and consequent uptake and intracellular redox cycling causing oxidative stress (3, 27). But seleno-L-cystine was less toxic, as expected, because after uptake, it must undergo enzymatic metabolic degradation by β-lyase to selenide to achieve its full toxic potential. In addition, part of the internalized selenocysteine might be secreted back to the extracellular compartment along the same pathway as cysteine. Further experiments demonstrated that the related selenium compounds seleno-L-methionine and selenate were nontoxic up to millimolar concentrations and that MSG and DTNB had no significant effects (data not shown). This was as expected, because both compounds exert low or no redox reactivity. The data suggest that selenate and seleno-L-methionine are much less preferable from a therapeutic standpoint, at least in the context of the mechanism for cancer-specific toxicity of redox active forms of selenium presented here.

In conclusion, we have proposed a novel model in which selenite and possibly other redox active forms of selenium should be considered prodrugs activated by the reductive microenvironment of malignant cells. The reductive microenvironment is in turn dependent on cystine uptake through the x_c^- antiporter, intracellular reduction by NADPH-dependent redox protein systems, and secretion of cysteine to the extracellular environment by MRPs (Fig. 6). The x_c^- antiporter, NADPH-dependent redox systems, and MRPs have been individually linked to tumor growth, progression, and multidrug resistance. Our findings highlight the unique therapeutic potential of reducible selenium compounds in treating cancer, especially in patients suffering from multidrug-resistant malignancies, along with the importance of and need for clinical trials in human subjects.

Materials and Methods

Chemicals. DTNB, GSH, TCEP, MSG, seleno-L-cystine, sodium selenite (Na_2SeO_3), the XTT viability kit, and DTT were all purchased from Sigma. RPMI medium, FBS, and penicillin-streptomycin (PEST) were obtained from Invitrogen. Thiolyte was purchased from Calbiochem, and GSSeSG was purchased from PharmaSe.

Cell Culture. All cells were grown in RPMI medium with 10% FBS and 1% PEST at 37 °C in a 5% CO_2 incubator. The main cell lines used were non–small cell lung carcinomas H157 and H611 and small cell lung carcinoma U2020 (28). For the verification experiment, the neuroblastoma-derived cell line SY-SH5Y and the hepatoma-derived cell line HUH7 (purchased from ECACC) were used. All experiments were adjusted for consistency.

Viability Measurements. Viability was measured by means of XTT in 96-well cell culture plates (Nunc). Cells were counted in a Burke's chamber, and 10,000 cells per well (200,000 cells/mL) were plated and preincubated for 20 h to allow adhesion. After preincubation, the medium was discarded, and treatments were applied in octuplets in 50 μL of fresh medium per well. After 20 h, 100 μL of mix, consisting of electron-coupling reagent (N-methyl dibenzopyrazine methyl sulfate), XTT labeling reagent, and fresh RPMI medium (1:50:50), was added to each well. The plate was read after 2 h at 470 nm (with 650 nm used as a reference and subtracted). Medium and reagent backgrounds were subtracted, and each data point was plotted relative to control cells.

Selenium Concentration Determination. Cells were split to three 75-cm^2 flasks per treatment, with 2.5 million cells per flask (200,000 cells/mL), and preincubated for 20 h to allow adhesion. Then the medium was removed, and cells were treated for 5 h with the treatment of choice in 12.4 mL of fresh medium. Cells were washed with PBS and harvested with trypsin, followed by centrifugation at 300 $\times$ *g* for 8 min, after which the medium was discarded. The resulting pellet was dissolved in 3 mL of Tris-HCl (100 mM) and sonicated for 4 $\times$ 10 s. Quantification of selenium was performed with inductively coupled plasma mass spectroscopy (29).

Medium Thiol Quantification. Total thiols in growth medium were quantified by extracting 400 μL of medium at different time points to end concentrations of 200 mM Tris-HCl (pH 8.0), 2 M guanidine hydrochloride, and 1 mM DTNB. Absorbance at 412 nm was measured spectrophotometrically (Ultrospec 4300 Pro).

HPLC for Reduced/Total Cysteine and GSH. HPLC was conducted as described by Luo et al. (30), but with an elution buffer pH of 3.76, not 3.71.

Western Blot Analysis for the xct Subunit. First, 50 μg of total protein per sample was loaded onto a 7.5% Tris-HCl gel (Bio-Rad) and run at 110 V for 1.5 h. The gel was then removed and placed in transfer buffer for 30 min. Transfer was conducted for 2 h using a Bio-Rad tank transfer. After transfer, the membrane was incubated in methanol for 15 min and then blocked with fat-free milk (5%) overnight. The membrane was washed 3 $\times$ 5 min in PBS-Tween and incubated with primary goat antibody against the xct subunit (Abcam; 1:1,000 dilution) for 2 h. The membrane was washed 4 $\times$ 5 min in PBS-Tween and incubated 1 h with HRP-conjugated mouse anti-goat secondary antibody (Dako; 1:2,000 dilution). The membrane was developed with a PerkinElmer Western Lightning Chemiluminescence Kit in Flourchem SP (Alpha Innotech).

Inhibition of MRP and Pgp. A total of 800,000 cells (200,000 cells/mL) were plated to 25-cm^2 cell flasks and left to adhere for 20 h. Then the medium was removed, and an equal volume of fresh medium with varying nontoxic concentrations of the inhibitors verapamil (Sigma) and MK571 (Calbiochem) was added. After 5 h, the thiol concentration was measured according to medium thiol quantification.

ACKNOWLEDGMENTS. This investigation was supported by grants from Cancerfonden (the Swedish Cancer Society), Cancer och allergifonden (the Swedish Cancer and Allergy Foundation), ALF (Stockholm County Council), and Radiumhemmets forskningsfonder.

1. Björkhem-Bergman L, et al. (2002) Drug-resistant human lung cancer cells are more sensitive to selenium cytotoxicity: Effects on thioredoxin reductase and glutathione reductase. *Biochem Pharmacol* 63:1875–1884.
2. Nilsonne G, et al. (2006) Selenite induces apoptosis in sarcomatoid malignant mesothelioma cells through oxidative stress. *Free Radical Biol Med* 41:874–885.
3. Kumar S, Björnstedt M, Holmgren A (1992) Selenite is a substrate for calf thymus thioredoxin reductase and thioredoxin and elicits a large non-stoichiometric oxidation of NADPH in the presence of oxygen. *Eur J Biochem* 207:435–439.
4. Yan L, Spallholz JE (1993) Generation of reactive oxygen species from the reaction of selenium compounds with thiols and mammary tumor cells. *Biochem Pharmacol* 45:429–437.
5. Lu J, Kaeck M, Jiang C, Wilson AC, Thompson HJ (1994) Selenite induction of DNA strand breaks and apoptosis in mouse leukemic L1210 cells. *Biochem Pharmacol* 47:1531–1535.
6. Rudolf E, Rudolf K, Cervinka M (2008) Selenium activates p53 and p38 pathways and induces caspase-independent cell death in cervical cancer cells. *Cell Biol Toxicol* 24:123–141.
7. Li J, Zuo L, Shen T, Xu CM, Zhang ZN (2003) Induction of apoptosis by sodium selenite in human acute promyelocytic leukemia NB4 cells: Involvement of oxidative stress and mitochondria. *J Trace Elem Med Biol* 17:19–26.
8. Zou Y, Niu P, Yang J, Yuan J, Wu T, Chen X (2008) The JNK signaling pathway is involved in sodium selenite–induced apoptosis mediated by reactive oxygen in HepG2 cells. *Cancer Biol Ther* 7:689–696.
9. Cavalieri RR, Scott KG, Sairenji E (1966) Selenite (75Se) as a tumor-localizing agent in man. *J Nucl Med* 7:197–208.
10. Tarze A, et al. (2007) Extracellular production of hydrogen selenide accounts for thiol-assisted toxicity of selenite against *Saccharomyces cerevisiae*. *J Biol Chem* 282:8759–8767.
11. Ganyc D, Self WT (2008) High-affinity selenium uptake in a keratinocyte model. *FEBS Lett* 582:299–304.
12. Lo M, Wang YZ, Gout PW (2008) The x(c)- cystine/glutamate antiporter: A potential target for therapy of cancer and other diseases. *J Cell Physiol* 215:593–602.
13. Griffith OW (1999) Biologic and pharmacologic regulation of mammalian glutathione synthesis. *Free Radical Biol Med* 27:922–935.
14. Saetre R, Rabenstein DL (1978) Determination of cysteine in plasma and urine and homocysteine in plasma by high-pressure liquid chromatography. *Anal Biochem* 90:684–692.
15. Banjac A, et al. (2008) The cystine/cysteine cycle: A redox cycle regulating susceptibility versus resistance to cell death. *Oncogene* 27:1618–1628.
16. Gout PW, Kang YJ, Buckley DJ, Bruchovsky N, Buckley AR (1997) Increased cystine uptake capability associated with malignant progression of Nb2 lymphoma cells. *Leukemia* 11:1329–1337.
17. Husbeck B, Nonn L, Peehl DM, Knox SJ (2006) Tumor-selective killing by selenite in patient-matched pairs of normal and malignant prostate cells. *Prostate* 66:218–225.
18. Sontheimer H (2004) Ion channels and amino acid transporters support the growth and invasion of primary brain tumors. *Mol Neurobiol* 29:61–71.
19. Lyons SA, Chung WJ, Weaver AK, Ogunrinu T, Sontheimer H (2007) Autocrine glutamate signaling promotes glioma cell invasion. *Cancer Res* 67:9463–9471.
20. Kim EH, et al. (2007) Sodium selenite induces superoxide-mediated mitochondrial damage and subsequent autophagic cell death in malignant glioma cells. *Cancer Res* 67:6314–6324.
21. Lo M, Ling V, Wang YZ, Gout PW (2008) The x_c^- cystine/glutamate antiporter: A mediator of pancreatic cancer growth with a role in drug resistance. *Br J Cancer* 99:464–472.
22. Dai Z, Huang Y, Sadee W, Blower P (2007) Chemoinformatics analysis identifies cytotoxic compounds susceptible to chemoresistance mediated by glutathione and cystine/glutamate transport system xc. *J Med Chem* 50:1896–1906.
23. Shih AY, et al. (2003) Coordinate regulation of glutathione biosynthesis and release by Nrf2-expressing glia potently protects neurons from oxidative stress. *J Neurosci* 23:3394–3406.
24. Surh YJ, Kundu JK, Na HK (2008) Nrf2 as a master redox switch in turning on the cellular signaling involved in the induction of cytoprotective genes by some chemopreventive phytochemicals. *Planta Med* 74:1526–1539.
25. Ceccarelli J, et al. (2008) The redox state of the lung cancer microenvironment depends on the levels of thioredoxin expressed by tumor cells and affects tumor progression and response to pro-oxidants. *Int J Cancer* 123:1770–1778.
26. Shen H, Yang C, Liu J, Ong C (2000) Dual role of glutathione in selenite-induced oxidative stress and apoptosis in human hepatoma cells. *Free Radical Biol Med* 28:1115–1124.
27. Björnstedt M, Kumar S, Holmgren A (1992) Selenodiglutathione is a highly efficient oxidant of reduced thioredoxin and a substrate for mammalian thioredoxin reductase. *J Biol Chem* 267:8030–8034.
28. Selenius M, Fernandes AP, Brodin O, Björnstedt M, Rundlöf AK (2008) Treatment of lung cancer cells with cytotoxic levels of sodium selenite: effects on the thioredoxin system. *Biochem Pharmacol* 75:2092–2099.
29. Larsen EH, et al. (2006) Uptake and speciation of selenium in garlic cultivated in soil amended with symbiotic fungi (mycorrhiza) and selenate. *Anal Bioanal Chem* 385:1098–1108.
30. -Luo JL, Hammarqvist F, Andersson K, Wernerman J (1998) Surgical trauma decreases glutathione synthetic capacity in human skeletal muscle tissue. *Am J Physiol* 275:E359–365.